

EUROPEAN SOUTHERN OBSERVATORY  
Organisation Européenne pour des Recherches Astronomiques dans l'Hémisphère Austral  
Europäische Organisation für astronomische Forschung in der südlichen Hemisphäre

**VERY LARGE TELESCOPE**

# **VISIR USER MANUAL**

R. Siebenmorgen, E. Pantin, M. Sterzik

Issue 1.1

10/12/04

**Change Record**

Issue/Rev.	Date	Section/Parag. affected	Reason/Initiation/Documents/Remarks
1.0	04/09/04	RSI, EPA, MST	First release for science verification in P74 and OT proposals in P75.
1.1	10/12/04	2.4, 3.2, 6.2, 6.3, 7, 8	update for P75 Phase2

## Contents

<b>1</b>	<b>Introduction</b>	<b>1</b>
<b>2</b>	<b>Observing in the MIR from the ground</b>	<b>1</b>
2.1	The Earth's atmosphere . . . . .	1
2.2	The spatial resolution . . . . .	1
2.3	MIR background . . . . .	4
2.4	Chopping and nodding . . . . .	4
2.5	Sensitivity . . . . .	4
<b>3</b>	<b>Instrument description and offered observing modes</b>	<b>4</b>
3.1	Imager . . . . .	5
3.2	Spectrometer . . . . .	6
3.3	Calibration units . . . . .	8
3.4	Detectors . . . . .	10
3.5	Data acquisition system . . . . .	12
<b>4</b>	<b>Observing with VISIR at the VLT</b>	<b>13</b>
4.1	Proposal preparation . . . . .	13
4.2	Telescope observing parameters . . . . .	14
4.3	Target acquisition . . . . .	15
4.4	Guide stars . . . . .	15
4.5	Brightness limitations . . . . .	15
4.6	Overheads . . . . .	15
4.7	Calibration observations . . . . .	15
<b>5</b>	<b>VISIR data</b>	<b>16</b>
5.1	Data format . . . . .	16
5.2	Pipeline . . . . .	17
5.3	VISIR spectrometer data . . . . .	17
<b>6</b>	<b>VISIR templates description</b>	<b>19</b>
6.1	Acquisition . . . . .	19
6.2	Observing with the imager . . . . .	19
6.3	Observing with the spectrometer . . . . .	21
6.4	Calibration . . . . .	22
<b>7</b>	<b>Appendix: VISIR template parameters</b>	<b>23</b>
7.1	Acquisition . . . . .	23
7.2	Observation . . . . .	24
7.3	Calibration . . . . .	26
<b>8</b>	<b>Appendix: Filter transmission curves</b>	<b>28</b>

## List of acronyms

BIB	Blocked impurity band
BLIP	Background limited performance
BOB	Broker of observation blocks
DIT	Detector integration time
ETC	Exposure time calculator
FWHM	Full width at half maximum
ICS	Instrument control software
IR	Infrared
IRACE	Infrared array control electronics
MIR	Mid infrared
OB	Observing block
P75	Period 75
P2PP	Phase 2 proposal preparation
PAE	Preliminary acceptance in Europe
pfov	pixel field of view
PSF	Point spread function
S/N	Signal-to-noise ratio
VISIR	VLT imager and spectrometer for the mid infrared
TCS	Telescope control system
TMA	Three mirrors anastigmatic
WCU	Warm calibration unit

## 1 Introduction

The VLT spectrometer and imager for the mid-infrared (VISIR), built by CEA/DAPNIA/SAP and NFRA/ASTRON, provides diffraction-limited imaging at high sensitivity in the two mid infrared (MIR) atmospheric windows: the N band between 8 to 13  $\mu\text{m}$  and the Q band between 16.5 and 24.5  $\mu\text{m}$ , respectively. In addition, it features a long-slit spectrometer with a range of spectral resolutions between 150 and 30000.

The MIR provides invaluable information about the warm dust and gas phase of the Universe. Micron sized particles such as silicates, silicon carbide, carbon, coals, aluminum oxides or polycyclic aromatic hydrocarbon (PAH) molecules are major contributors to the thermal MIR emission. The gaseous phase emits through a large number of ionic and atomic lines. Examples are NeII (12.8  $\mu\text{m}$ ) and the pure rotation lines of molecular hydrogen at 8.02, 9.66, 12.27 and 17.03  $\mu\text{m}$ .

Because of the very high background from the ambient atmosphere and telescope, the sensitivity of ground-based MIR instruments cannot compete with that of space-born ones. However, ground based instruments mounted on large telescopes offer superior spatial resolution. For example VISIR at the VLT provides diffraction limited images at  $\sim 0.3''$  (FWHM) in the N band. This is an order of magnitude better than what can be reached by the Spitzer Space Telescope (SST).

The VISIR user manual is structured as follows: Basic observing techniques of ground-based MIR instruments are summarized in Sect. 2. A technical description of VISIR and its observing modes offered for period 75 (P75) are given in Sect. 3. An overview on how to observe with VISIR at the VLT can be found in Sect. 4. Acquisition, observing and calibration templates are explained in Sect. 6.

This manual reflects knowledge gathered during early phases of operations and is in some aspects to be considered to be preliminary. Therefore we strongly recommend to consult:

<http://www.eso.org/instruments/visir/> for additional information and updates. Further support during proposal preparation and OB submission please contact ESO's User Support Group ([usg-help@eso.org](mailto:usg-help@eso.org)).

## 2 Observing in the MIR from the ground

### 2.1 The Earth's atmosphere

Our atmosphere absorbs the majority of the MIR radiation from astronomical sources. The main absorbing molecules are  $\text{H}_2\text{O}$ ,  $\text{CH}_4$ ,  $\text{CO}_2$ ,  $\text{CO}$ ,  $\text{O}_2$ ,  $\text{O}_3$ . However, the atmosphere is quite transparent in the two atmospheric windows: the N and Q band. They are centered around 10 and 20  $\mu\text{m}$ , respectively. The transmission in the N band is fairly good at a dry site and becomes particularly transparent in the wavelength range 10.5-12  $\mu\text{m}$ . However, the transmission of the Q band is rapidly decreasing with wavelength and can be viewed as the superposition of many sub-bands having a typical spectral coverage of  $\Delta\lambda = 1\mu\text{m}$  at an average transmission of 60%. Observations in this band require low water vapor content in the atmosphere. The atmospheric transmission in the N and Q bands is displayed on Fig. 1.

### 2.2 The spatial resolution

The spatial resolution of an instrument is ultimately limited by diffraction of the telescope and the atmospheric seeing. The diffraction limit increases with wavelength as  $1.22 \lambda/D$ , where  $\lambda$  is the observing wavelength and  $D$  the diameter of the telescope mirror. The wavelength dependence of the seeing can be derived by studying the spatial coherence radius of the atmosphere in the telescope beam and is to first order approximated by the Roddier formula, where the seeing is  $\propto \lambda^{-0.2}$ . However, initial results from VISIR data indicate that this formula overestimates the measured MIR seeing at Paranal by 20-50%. As a result, VISIR data are already diffraction limited for optical seeing below  $0.6''$ .

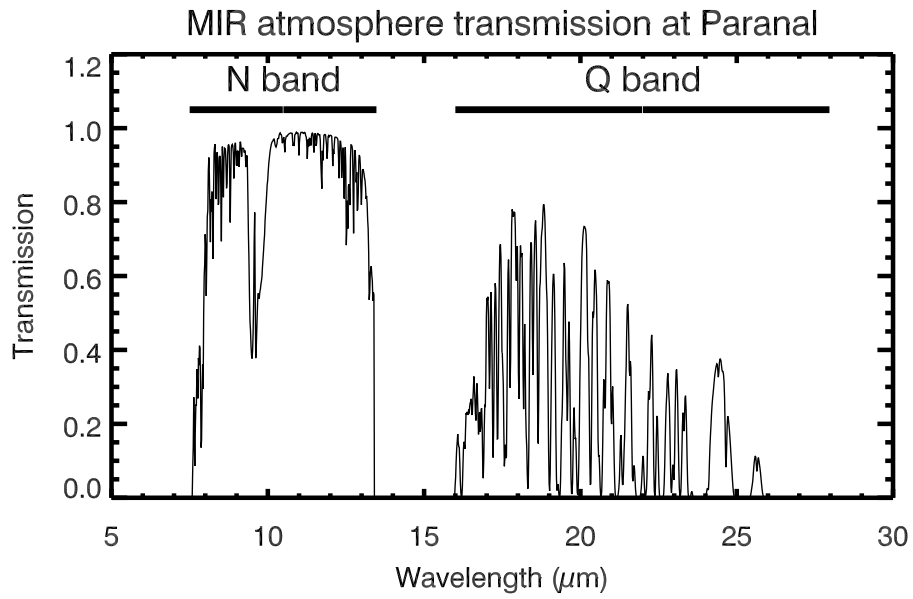


Figure 1: MIR atmospheric transmission at Paranal computed with HITRAN for an altitude of 2600 m and 1.5 mm of precipitable water vapor at zenith. The US standard atmosphere is used.

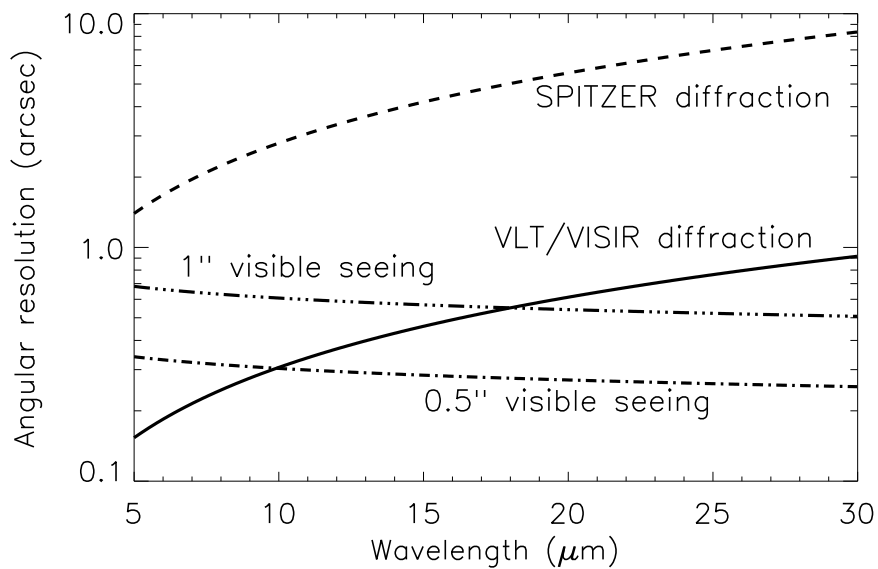


Figure 2: VLT diffraction limit (full line) versus seeing. SST diffraction limits (dashed) are shown for comparison. The Roddier dependence is shown for two optical seeings (dashed-dot).

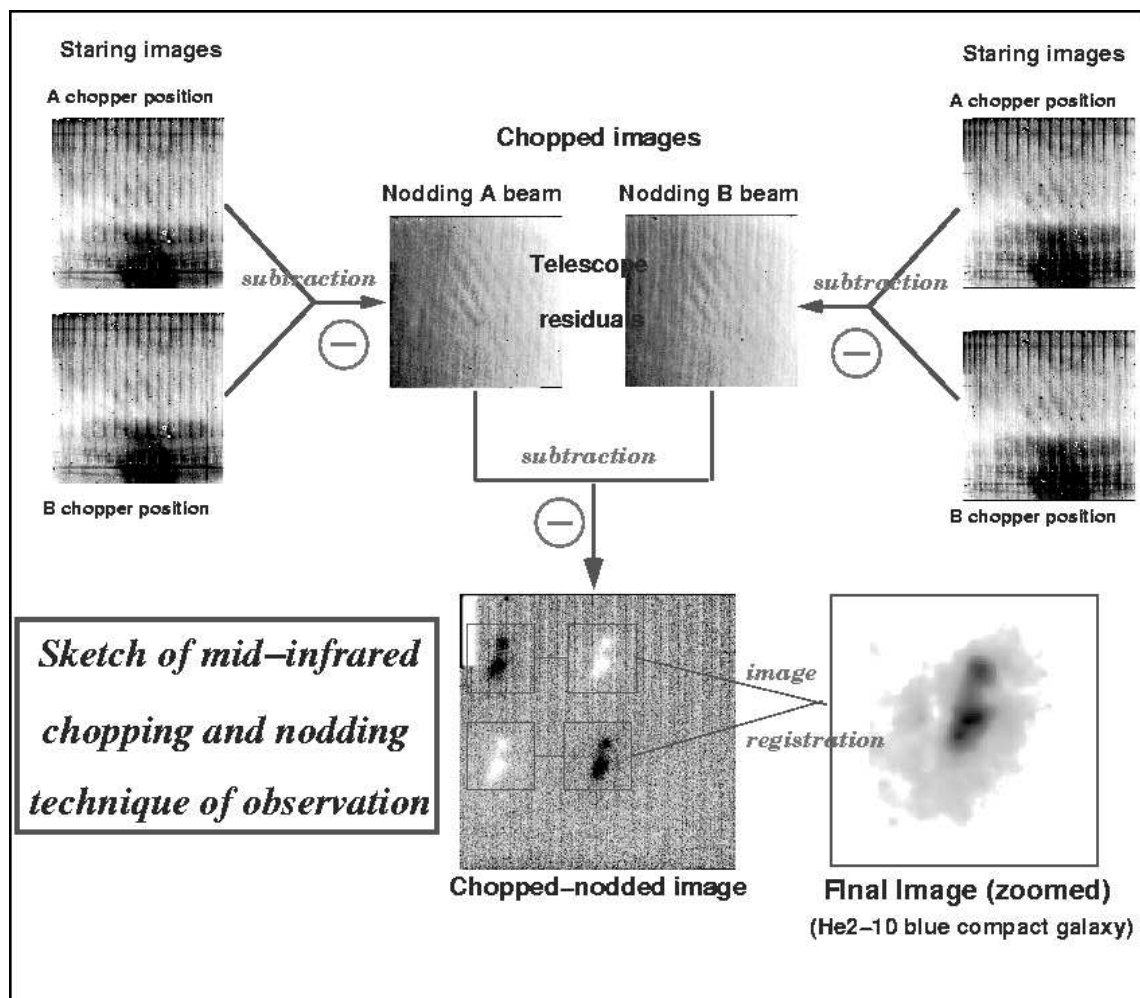


Figure 3: Illustration of the chopping and nodding technique on observations of the blue compact galaxy He2-10. The galaxy only appears after chopping and nodding (courtesy VISIR commissioning team, June 2004)

## 2.3 MIR background

The atmosphere does not only absorb MIR photons coming from astrophysical targets, but also emits a strong background with the spectral shape of a black-body at about 253 K (Kirchhoff's law). The telescope gives an additional MIR background. The VLT telescopes emit at 283 K with a preliminary emissivity estimate of  $< 15\%$ . The VISIR instrument is cooled to avoid internal background contamination. The detectors are at  $\sim 7$  K and the interior of the cryostat at 33 K. The background radiation at  $10\mu\text{m}$  is typically  $m_N = -5 \text{ mag/arcsec}^2$  ( $3700 \text{ Jy/arcsec}^2$ ) and at  $20\mu\text{m}$   $m_Q = -7.3 \text{ mag/arcsec}^2$  ( $8300 \text{ Jy/arcsec}^2$ ).

## 2.4 Chopping and nodding

The basic idea to suppress the MIR background is to perform differential observations. In the so-called chopping technique two observations are performed. One set of exposures on-source, include the background and the astronomical source. The second set of exposures off-source measures the pure background. The on and off source observations have to be alternated at a rate faster than the rate of the background fluctuations. For VISIR at Paranal, a chopper frequency of 0.25 Hz has been found to be adequate for N-band imaging observations, while 0.5 Hz are adopted for Q-band imaging. Spectroscopic observations are performed with even lower chopper frequencies, at 0.1 Hz. Switching from on to off source and vice versa is achieved by moving the secondary mirror of the telescope. The chopping technique cancels most of the background. However, the optical path is not exactly the same in both chopper positions. Therefore a residual background remains. It is varying at a time-scale which is long compared to that of the sky. This residual is suppressed by nodding, where the telescope itself is moved off source and the same chopping observations as in the on source position is repeated. An illustration of the chopping and nodding technique is shown on Fig. 3. Depending on the choice of chopping and nodding amplitudes and directions, typically 4 images of the source can be seen on the frame and used for scientific analysis.

## 2.5 Sensitivity

The sensitivity of the VISIR imaging observing modes is typically a factor 2–3 above the one expected from the photon noise originating from the background. The sensitivities measured during commissioning of the VISIR filters offered in P75 are shown in Table 2. Sensitivity limits are determined by observing calibration standard stars and extrapolated to estimate the limiting flux expected in one hour on source integration of a point-source detected with a S/N of 10. Sensitivity estimates of VISIR spectroscopy observing modes are given in Table 4 – 6. As an example in Fig. 4 the sensitivity limit of the low resolution mode in the N band is given. The sensitivity limits are the basis to assess the feasibility of an observing programme. For up to date information, please consult <http://www.eso.org/instruments/visir> and use the VISIR exposure time calculator (ETC, located at <http://www.eso.org/observing/etc/>) to estimate the observing time.

## 3 Instrument description and offered observing modes

Imaging and long-slit spectroscopy with VISIR can be achieved at several spatial and spectral resolution. The imager and spectrograph are two sub-instruments. They have independent light paths, optics and detectors. The spectrometer has two arms, one with low order gratings for the low and medium spectral resolution, the other with large echelle gratings providing high spectral resolution. The cryogenic optical bench is enclosed in a vacuum vessel. The vessel is a cylinder, 1.2 m long and 1.5 m in diameter. Standard Gifford–McMahon closed-cycle coolers are used to maintain the required temperature: 33 K for most of the structure and optics and  $< 15$  K for the parts near the detector. The detectors are cooled down to  $\sim 7$  K.



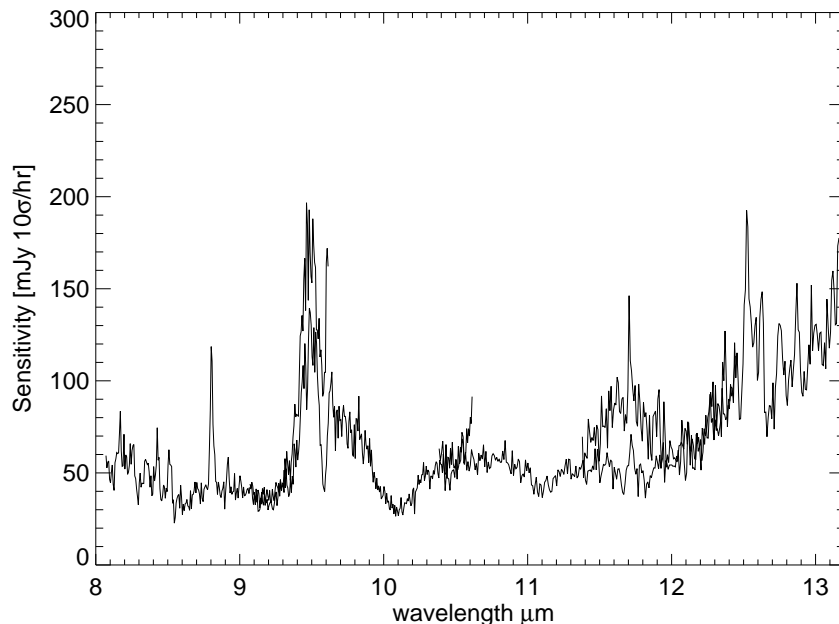


Figure 4: One example of the wavelength dependence of the sensitivity limit of the VISIR low resolution spectroscopic mode. The four offered settings of the N band are stitched together. Due to the interference of atmospheric molecular absorption, e.g. at 9.55, 11.8 and 12.5  $\mu\text{m}$ , the S/N and hence the sensitivity limit, becomes a function of wavelength. Note the detector feature at 8.8  $\mu\text{m}$ .

### 3.1 Imager

The imager is based on an all-reflective design. The optical design is shown in Fig. 5. It consists of two parts:

- A collimator, which provides an 18 mm cold stop pupil in parallel light. As generally designed for IR instruments, the pupil of the telescope is imaged on a cold stop mask to avoid straylight and excessive background emission. The collimator mirror (M1) is a concave aspherical mirror. It is followed by a folding flat mirror (M2) which eases the mechanical implementation.
- A set of three objectives mounted on a wheel. Each objective is based on a three mirror anastigmatic (TMA) system. Each of the TMA's is made of three conic mirrors.

The 0.075'' and 0.127'' pixel scale are offered in P75 (Table 1) in the future it is planned to commission a larger pixel scale as well. The offered pfov ensure a proper sampling of the images in the N and Q band.

pfov	fov	diffraction <sup>a</sup> $\mu\text{m}$	diffraction <sup>a</sup> pixels
0.127''	32.5'' $\times$ 32.5''	94	1.88
0.075''	19.2'' $\times$ 19.2''	159	3.18

<sup>a</sup> Radius of first Airy ring at  $\lambda=7.7\mu\text{m}$

Table 1: VISIR imager pixel scales offered in P75. The pixel size of the DRS 256x256 detector is 50  $\mu\text{m}$ . The first airy ring at  $\lambda=7.7\mu\text{m}$  corresponds to an radius of 0.24'' on the sky.

The filter wheel is located just behind the cold stop pupil mask. The list of filters offered in P75 is given in Table 2. The transmission curves of the filters measured at 35 K are plotted in the Appendix.

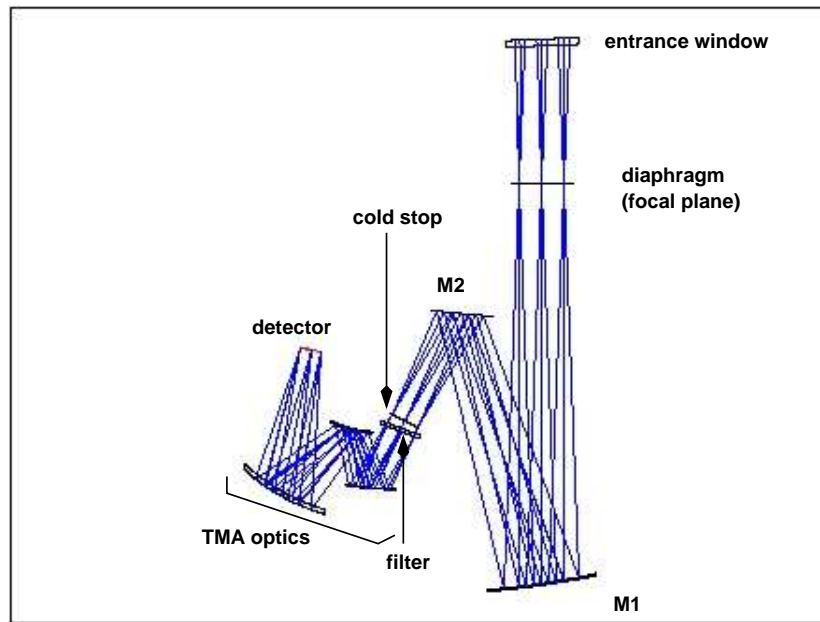


Figure 5: The optical path of the imager in the intermediate field ( $0.127''/\text{pixel}$ ) is shown from the entrance window down to the detector.

### 3.2 Spectrometer

VISIR offers long-slit spectroscopy at three spectral resolutions with pixel scale of  $0.127''$  and slit length of  $32.28''$ . The all-reflective optical design of the spectrometer uses two TMA systems in double pass (pass 1: collimator, pass 2: camera). A schematic layout of the VISIR spectrometer design is shown in Fig. 6. The 3-mirror system of the low- and medium-resolution arm gives a 53 mm (diameter) collimated beam; the collimated beam diameter in the high-resolution arm is 125 mm. Both subsystems image the spectrum onto the same detector; selection between the two spectrometer arms is done by two pairs of folding flat mirrors. In front of the actual spectrometer subsystems is a reflective re-imager consisting of two off-axis paraboloids and three folding flats. The re-imager provides a 16 mm (diameter) cold-stop pupil in parallel light and transforms the incoming VLT Cassegrain beam of F:13.4 to an F:10 beam at the spectrometer entrance. The spectrometer slit wheel is also equipped with a very wide slit ( $15.3''$ ) giving the possibility to make imaging with the spectrometer detector. This is used for object acquisition and centering on the detector.

The list of available filters for spectroscopic acquisition offered in P75 is given in Table 3, together with their measured bandpasses and approximate sensitivities for image acquisition.

In P75, three different slit widths ( $0.4''$ ,  $0.75''$  and  $1''$ ) are offered for all settings. For over-sized widths (e.g. for the  $1''$  slit with respect to the diffraction limit around  $10\mu\text{m}$ ) the resolution is degraded by  $\sim 30\%$  with respect to the theoretical limit. In the N band, the low-resolution has a spectral resolving power  $\sim 300$  (Table 4) and the medium-resolution  $\sim 3000$  (Table 5), respectively. In P75 two settings of the medium resolution mode at  $8.8$  and  $11.4\mu\text{m}$  are commissioned. In high resolution a narrow wavelength range around the  $12.813\mu\text{m}$  [Ne II] line is offered, and only in long-slit mode. With the [Ne II] order selection filter central wavelengths between  $12.738$  and  $12.882\mu\text{m}$  are accessible. The spectral resolution varies with wavelength and may reach up to  $R \sim 30000$  for the smallest slits. With the  $1''$  slit the measured spectral resolution is  $R \sim 15000$  (Table 6). Note that in the high resolution

filter	$\lambda$ – center ( $\mu\text{m}$ )	half-band width ( $\mu\text{m}$ )	maximum transmission (%)	sensitivity ( $\text{mJy}/10\sigma/1\text{h}$ )
PAH1	8.59	0.42	77	20
ArIII	8.99	0.14	72	25
SIV_1	9.82 <sup>1</sup>	0.18	72	50
SIV	10.49	0.16	70	20
SIV_2	10.77 <sup>1</sup>	0.19	70	40
PAH2	11.25	0.59	75	20
SiC	11.85	2.34	75	30
PAH2_2	11.88 <sup>1</sup>	0.37	58	35
NeII_1	12.27 <sup>1</sup>	0.18	51	50
NeII	12.81	0.21	64	40
NeII_2	13.04	0.22	68	50
Q1	17.65	0.83	59	400
Q2	18.72	0.88	49	250
Q3	19.50	0.40	50	400

Table 2: VISIR imager filter characteristics (manufacturer specifications) and measured sensitivities.  
<sup>1</sup> determined with a monochromator and the WCU, because deviates from specifications.

filter	$\lambda$ – center ( $\mu\text{m}$ )	half-band width ( $\mu\text{m}$ )	maximum transmission (%)	sensitivity ( $\text{mJy}/10\sigma/1\text{h}$ )
N_SW	8.85	1.35	n.d.	40
N_LW	12.1	1.9	n.d.	40
ArIII	8.94	0.11	n.d.	200
NeII_1	12.35	0.50	n.d.	80
NeII_2	12.81	0.10	n.d.	50

Table 3: VISIR spectrometer filter characteristics and measured sensitivities. The filters transmissions have been determined with a monochromator and the WCU.

mode a minimum flux in the line of  $3 \cdot 10^{-16} \text{ W/m}^2/\text{arcsec}^2$  is required. This value corresponds to an approximate sensitivity limit of 5 Jy in the continuum.

Please consult <http://www.eso.org/instruments/visir> for the latest update of the list of offered modes and slits.

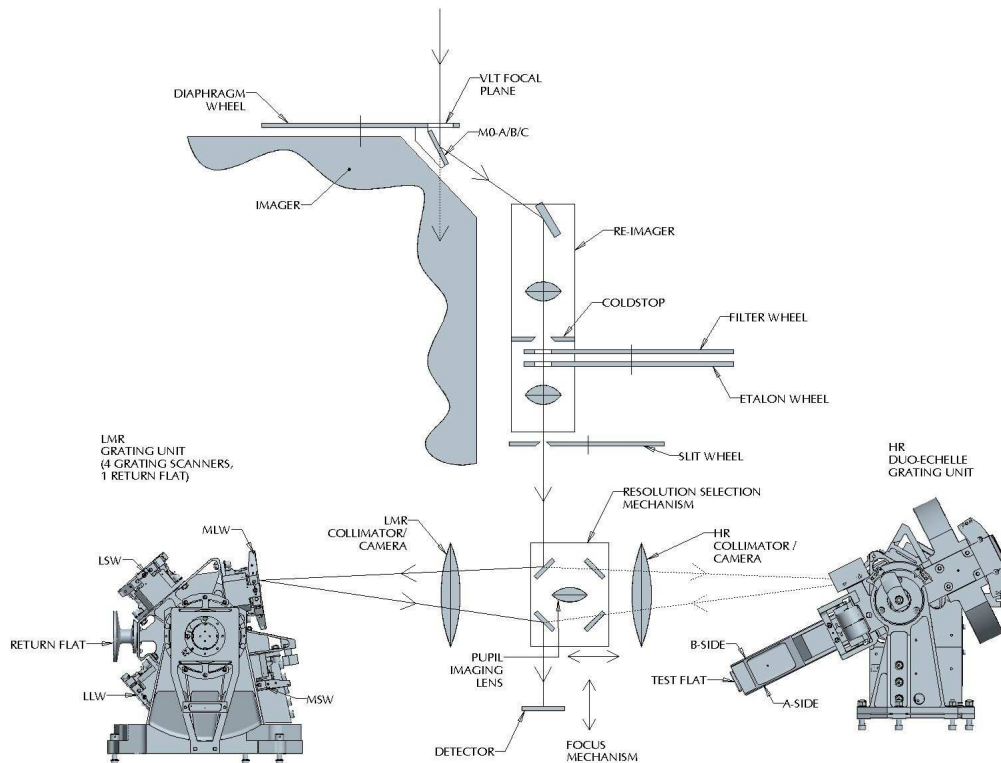


Figure 6: Schematic layout of the design of the VISIR spectrometer.

$\lambda$ - range ( $\mu\text{m}$ )	$\lambda$ - center ( $\mu\text{m}$ )	grating order	spect.-resol. (measured, 1"slit)	dispersion (pixels/ $\mu\text{m}$ )
8.0-9.6	8.8	2	300 - 390	160.02
9.0-10.6	9.8	2	305 - 360	160.05
10.34-12.46	11.4	1	185 - 220	119.94
11.34-13.46	12.4	1	215 - 250	119.96

Table 4: VISIR low resolution setting. The measured sensitivities are  $\sim 50 \text{ mJy}/10\sigma/1\text{h}$  (cf. Fig. 4).

### 3.3 Calibration units

A warm calibration unit (WCU) is located on top of the VISIR vacuum enclosure. The WCU is also called star simulator. It simulates either a monochromatic point source with adjustable wavelength or an extended black-body source with adjustable temperature. A selection mirror allows to switch from the telescope to the simulator beam. It can be used for calibration and tests, also during daytime. Fig. 7 shows the unit on top of the enclosure.

$\lambda$ - range ( $\mu\text{m}$ )	$\lambda$ - center ( $\mu\text{m}$ )	grating order	spect.-resol. (measured, 1"slit)	dispersion (pixels/ $\mu\text{m}$ )
8.706-8.893	8.8	2	$\sim 3500$	1367.43
11.274-11.526	11.4	1	1640 - 1970	1011.2

Table 5: VISIR medium resolution setting. The measured sensitivities are  $\sim 200 \text{ mJy}/10\sigma/1\text{h}$ .

$\lambda$ - range ( $\mu\text{m}$ )	$\lambda$ - center vacuum ( $\mu\text{m}$ )	line	order	spect.-resol. (measured, 1"slit)	dispersion (pixels/ $\mu\text{m}$ )
12.738-12.882	12.81	[Ne II]	11A	12910 - 15490	7124.74

Table 6: VISIR high resolution mode. The measured sensitivities is estimated to be  $\sim 5 \text{ Jy}/10\sigma/1\text{h}$ .

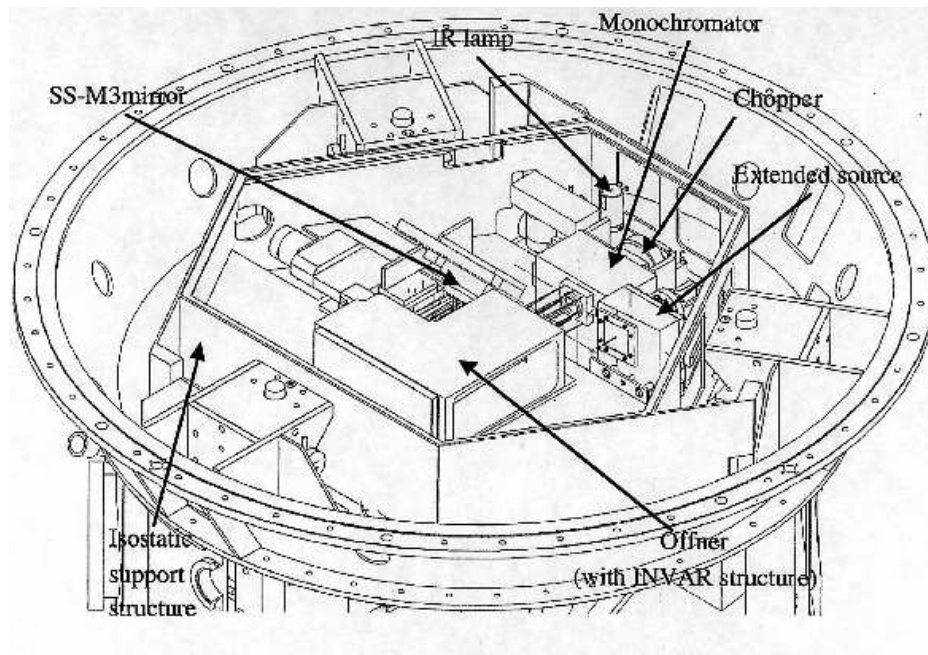


Figure 7: Schematic drawing of the warm calibration unit on top of the VISIR vessel.

### 3.4 Detectors

The VISIR imager and spectrometer are each equipped with a DRS, former Boeing,  $256 \times 256$  BIB detector. The quantum efficiency of the detectors is greater than 50% and reaches 65% or more at  $12 \mu\text{m}$  (Fig. 8). The detector noise has to be compared with the photon noise of the background. As shown in Fig. 9, the measured noise in an observation consists of read-out noise and fixed pattern noise, which are both independent of the detector integration time (DIT). At the operating temperature of the detector ( $\sim 7\text{K}$ ), the dark current, which is the signal obtained when the detector receives no photons, is negligible compared to the background generated by the photons emitted by the telescope and the atmosphere. The dark current is removed by the observation technique (chopping or nodding). It is at least 6 times lower than the photon noise for the spectrometer and negligible for the imager. The detectors have a switchable pixel (“well”) capacity. The large capacity is used for broad-band imaging and the small capacity for narrow band imaging and spectroscopy. Detector saturation due to the enormous MIR background is avoided by a storage capacity of  $1.9 \cdot 10^6 \text{ e}^-$  in small and  $1.8 \cdot 10^7 \text{ e}^-$  in large capacity modes, respectively. For background limited noise performance (BLIP), the optimal operational range of the detector is half of the dynamic range for the large capacity, and between 1/2 and 1/5 for the small capacity. The detector is linear over 2/3 of its dynamic range (Fig. 10) and its working point is set in the middle of the dynamic range. During commissioning it was found that, for about half of the array, the gain does not differ by more than 2% peak-to-peak. By comparison with other limitations, flat-field corrections, which are difficult to implement in the MIR, are not considered important. The detector integration time (DIT) is a few milli-seconds in broad-band imaging and may increase to  $\sim 2\text{ s}$  in high resolution spectroscopy. The DIT is determined by the instrument software according to the filter and pfov. It is not a parameter to be chosen by the observer. The DRS detectors contain a fair fraction of bad pixels ( $< 2\%$ , Fig.11). The imager detector also suffer from striping and appearances of ghosts. These artifacts are smaller in spectroscopy due to the lower light levels but clearly visible on objects brighter than  $\sim 2\%$  of the background or by reading hot pixels. The relatively wide rectangular area in the upper left corner of the imager detector or some other rectangular areas are masked out to avoid such disturbances (Fig. 12). For bright objects the DRS detector shows memory effects. Stabilization is ensured by introducing dead times where necessary. It is advised to observe only sources fainter than  $500\text{ Jy}$  in N and  $2500\text{ Jy}$  in Q.

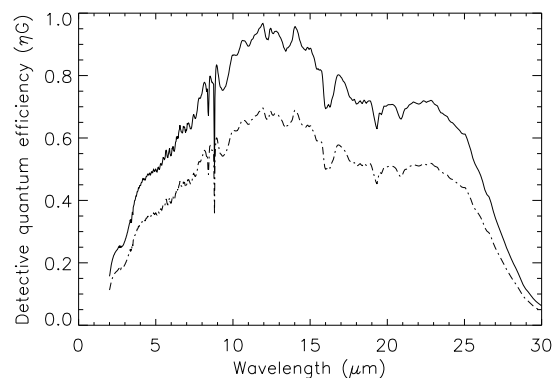


Figure 8: Detector quantum efficiency at 12K provided by DRS (solid line). The same curve (dashed) but scaled by 0.72 reflects a lower limit of the quantum efficiency. The scaling was derived from laboratory measurements. Note the sharp absorption feature at  $8.8 \mu\text{m}$  that will appear in raw spectroscopic data.

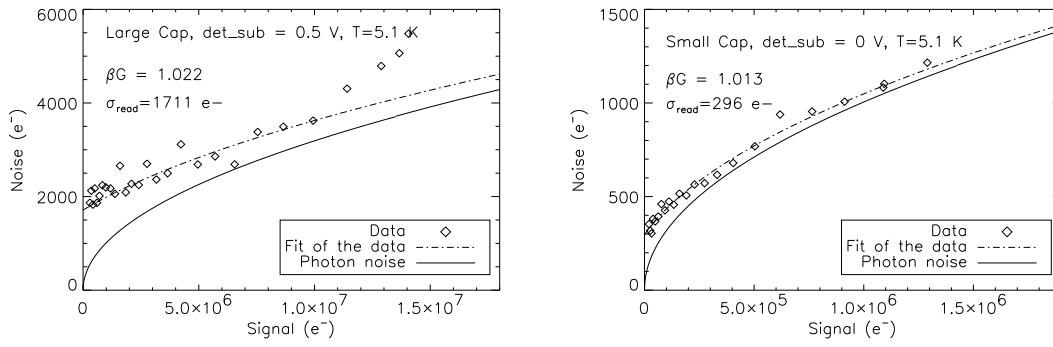


Figure 9: Noise as a function of the incoming flux in the large (left) and small (right) capacity mode. Superimposed is the theoretical photon noise. BLIP performances are approached for higher fluxes and larger DIT, respectively.

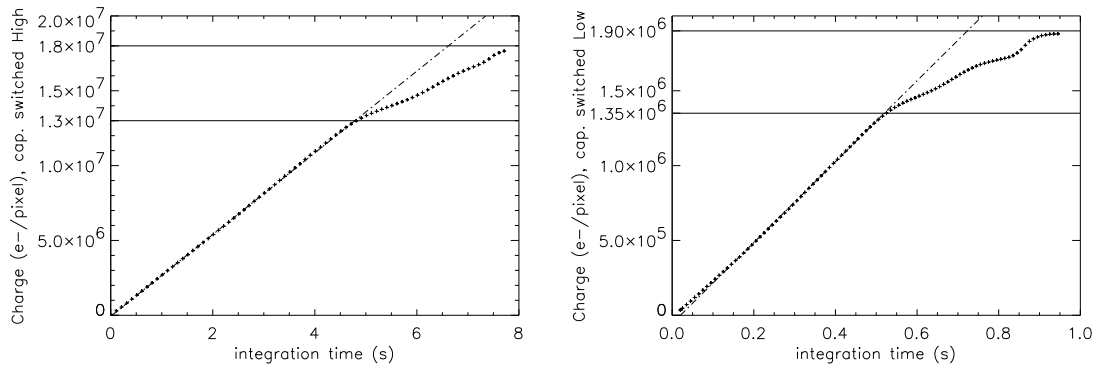


Figure 10: Linearity curve of the detector in the large (left) and small (right) capacity modes. The break in the response at  $\approx 2/3$  at  $1.8 \cdot 10^7 e^-$  of the large and at  $1.9 \cdot 10^6 e^-$  of the small capacity are indicated by full lines. The top lines indicate the well capacities.

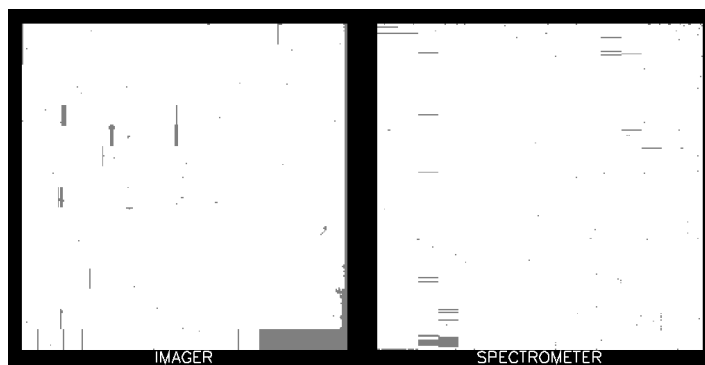


Figure 11: Bad pixel maps of the imager and the spectrometer detector. The large grey rectangular areas correspond to electronically masked pixels in order to avoid detector striping.

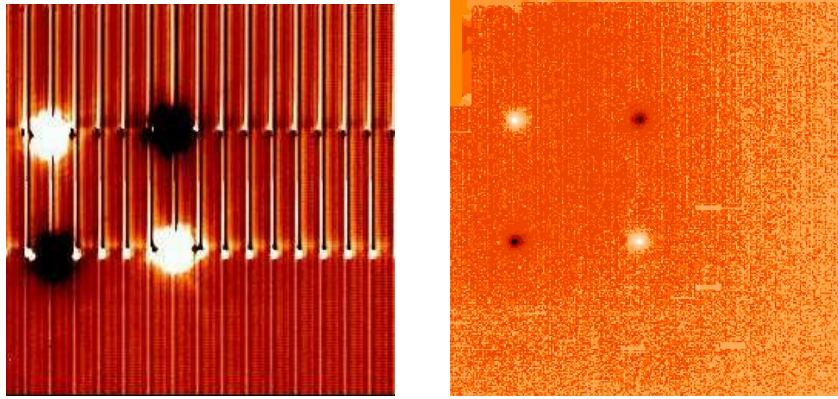


Figure 12: The DRS detector shows stripes and repeating ghosts for very bright sources (left). The ghosts are distributed every 16 columns. For other sources striping is not apparent (right).

### 3.5 Data acquisition system

The VISIR detectors are both controlled by the ESO standard IRACE acquisition system. In imaging the read-out rate of the detector is high. Up to 200 frames per s are read for a minimum detector integration time of  $DIT = 5$  ms. Such a frame rate is too high to store all exposures. One VISIR image is of size  $256 \times 256$ ; each pixel is coded with 4 bytes (long integer). Thus one read-out has a size of 262 kB. During each chopping cycle the elementary exposures are added in real time and only the result is stored on disk. At a chopping frequency of  $f_{\text{chop}} = 0.25$  Hz every  $T_{\text{chop}} = 4$  s one VISIR image is stored as a plane in a data cube of a FITS file. The number of chopping cycles corresponds to the time spent in one nodding position,  $T_{\text{nod}}$ . This nodding period is typically  $T_{\text{nod}} = 90$  s for science observations. The chopper frequency, DIT and also  $T_{\text{nod}}$  are predefined by the system. The number of saved A–B frames in one FITS file is:

$$N_{\text{cycl\_chop}} = T_{\text{nod}}/T_{\text{chop}} \quad (1)$$

The number of nodding cycles is computed from the total integration time as given by the observer. The total number of stacked images for each secondary position, respectively chopper half cycle, is NDIT. This parameter is computed according to:

$$\text{NDIT} = (2 \cdot \text{DIT} \cdot f_{\text{chop}})^{-1} - \text{NDITSKIP} \quad (2)$$

and is given by the system. It depends on DIT, chopping frequency and NDITSKIP: some read-outs at the beginning of each chopper half cycle are rejected during stabilization of the secondary. Typical stabilization times of the secondary are 25 ms. The number of rejected exposures is given by NDITSKIP. Similar, during stabilization after each telescope movement, respectively nodding position, a number NCYSKIP of chopping cycles is ignored. The timing organization of data is shown in Fig. 13.

The total on source integration time is:

$$t_{\text{source}} = 4 \cdot N_{\text{cycl\_nod}} \cdot N_{\text{cycl\_chop}} \cdot \text{NDIT} \cdot \text{DIT} \quad (3)$$

The total rejected time is:

$$t_{\text{skip}} = 4 \cdot N_{\text{cycl\_chop}} \cdot \text{DIT} \cdot (\text{NDITSKIP} \cdot N_{\text{cycl\_nod}} + \text{NDIT} \cdot \text{NCYSKIP}) \quad (4)$$

and the total observing time is:



$$t_{\text{tot}} = t_{\text{source}} + t_{\text{skip}} \quad (5)$$

Typical duty cycles ( $t_{\text{source}}/t_{\text{tot}}$ ) are about 70%.

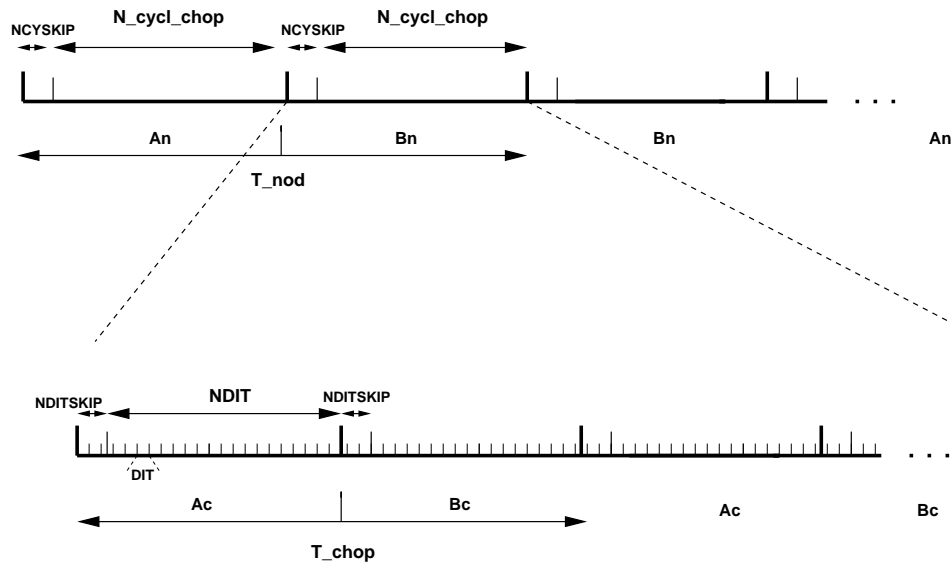


Figure 13: Data timing in VISIR.  $A_c$  and  $B_c$  refer to the two chopper positions,  $A_n$  and  $B_n$  refer to the two nodding (telescope) positions. Note the  $A_n B_n B_n A_n$  cycle sequence for the nodding to save observing time.

## 4 Observing with VISIR at the VLT

### 4.1 Proposal preparation

Tools are available to prepare the observations, either during phase I, call for proposals, or during phase II, when observing blocks are created by the observer. The exposure time calculator (ETC available at <http://www.eso.org/observing/etc/>) may be used to estimate the integration time needed to obtain the required S/N for a given instrument setting. As for all VLT instruments, astronomers with granted VISIR telescope time prepare their observations using the phase two proposal preparation tool (P2PP), described at <http://www.eso.org/observing/p2pp/P2PP-tool.html>. Acquisitions, observations and calibrations are coded via observing templates. One or more templates build up an observing block (OB). They contain all the information necessary for the execution of a complete observing sequence. An overview of the available VISIR templates and their parameters is given in Sect. 5 of this manual. For each science template, the user has to provide a finding chart so that the target can be acquired. In addition to the general instruction on how to create these finding charts, see <http://www.eso.org/observing/p2pp/ServiceMode.html>, the following VISIR requirements apply:

- All finding charts have to be made using existing infrared (K-band or longer wavelength) images. Typically, 2MASS or DENIS K-band images are acceptable, although higher spatial resolution may be preferable.
- If the wavelength at which the finding chart has been taken is different from that of the science observation, e.g. a K-band finding chart for a  $10\mu\text{m}$  spectroscopic template, the user has to describe clearly how to identify the target at the observing wavelength in the README section of the programme description. Adequate examples of such comments are:

- The target will be the brightest source in the field of view at  $10\mu\text{m}$  .
- At  $10\mu\text{m}$  , there will be two bright sources in our field of view. The science target is the southernmost of these two.

Important note:

1. In service mode it is mandatory to specify a guide star brighter than  $V=12$  within a field of  $5'$  radius around the science target.
2. All observations can be performed in service mode. Visitor mode in P75 will be granted in exceptional cases and requires special justification.

## 4.2 Telescope observing parameters

The chopping technique, as described in Sect. 2, is based on beam switching using a moving secondary mirror of the telescope. It allows to alternatively observe a field, then another field offset from the first by a chopping distance or throw, called `CHOP.THROW`. To avoid chopping inside the object it is recommended to use a chopping and nodding throw which is  $\sim 1.5$  times larger than the estimated MIR diameter of the object. In the case of point sources, the throw is usually set around  $\sim 10''$  to ensure proper separation of the different beams. The maximum chopping throw at the VLT is  $30''$  and the minimum is  $8''$ . Note that for chopping throws larger than the field-of-view, the negative beams will not be seen on the detector, and the integration times have to be adjusted accordingly. As stated in Sect 3.5, the chopping frequency is not a parameter accessible to the observer, it is fixed internally to ensure the best data quality. However, chopper throw and position angle, `TEL.CHOP.POSANG`, which is the angle of chopping with respect from the North to East are parameters to be set by the observer. The definition of both parameters are described in Fig. 14. Note that `TEL.CHOP.POSANG` (similar as `TEL.ROT.OFFANGLE`) is equal to the *negative* of the astronomical position angle  $PA$  on sky. The nodding technique allows to switch from one field to another by offsetting the telescope by several tens of arc-seconds. The nodding period is typically 30 s. It allows to correct for optical path residuals that remain after chopping (Sect. 2). Most nodding offsets are implicitly set with respect to the chopping throw value.

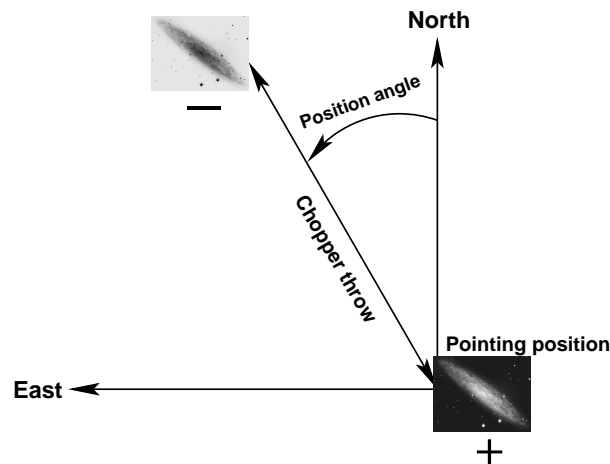


Figure 14: Definition of chopping parameters. The position angle ( $PA$ ) is measured counter-clockwise from North to East, `TEL.CHOP.POSANG` is  $-PA$ .

### 4.3 Target acquisition

Observing blocks must start with an acquisition template. Pointing to a target can only be performed through an acquisition template. Target coordinate, name, proper motion are set in the acquisition templates. The execution of the acquisition templates presets the telescope to the target coordinate and starts an imaging exposure using the most sensitive configuration. Then, the target, once localized in the field, can be offset to a particular position onto the detector or in the slit. There are two acquisition templates for imaging, `VISIR_img_acq_Preset`, `VISIR_img_acq_MoveToPixel` and one for spectroscopy, `VISIR_spec_acq_MoveToSlit`. The observing parameters are described in Sect.7.1. In P75, acquisition is limited to objects brighter than 0.2 Jy. This limit has to be considered especially for VISIR spectroscopic observations, because VISIR imaging modes it is possible to perform blind preset observations with `VISIR_img_acq_Preset` template followed by a deeper integration. Acquisition images are recorded except for blind presets.

### 4.4 Guide stars

Guide stars are automatically selected by the TCS from the guide star catalog or are provided by the observer. The telescope operator acknowledges the selected star. Guide stars are mandatory for active optics and field stabilization. Any VLT programme should make sure that it is possible to find a guide star (USNO catalog) with a  $V = 11 - 13$  mag within a field of 5' around the object.

### 4.5 Brightness limitations

There are currently no brightness limitations with VISIR. However, it is advised to observe only sources fainter than 500 Jy in N and 2500 Jy in Q to avoid detector artifacts (Sect. 3.4).

### 4.6 Overheads

The VLT telescope overhead for one OB which includes active optics setting, selection of guide star, field stabilization is 6 min.

VISIR instrument configurations can be changed in a short time. For example a complete change of instrument settings takes less than 2 minutes. The total time for an image acquisition of a bright sources ( $> 1$  Jy) takes  $\sim 5$  min. for one fine acquisition iteration, or in blind preset 2 min. Spectroscopic acquisitions take longer and are strongly dependent on the source brightness : an overhead of 15 min. is accounted for sources  $> 1$  Jy, while 30 min. are required for sources between 0.2 and  $> 1$  Jy, respectively.

Instrument overheads due to chopping and nodding duty cycle losses have been measured to be 25% of the observing time for the imager and 50% for the spectrometer, respectively.

The total observing time requested by the observer must include telescope and instrument overheads.

### 4.7 Calibration observations

MIR observations depend strongly on the ambient conditions such as humidity, temperature or air-mass. In service mode science observations are interlace by calibration observations on a timescale of 3h. Observations of photometric standards will be provided by the observatory within a time interval of three hours w.r.t. the science observations. Calibrators, unless provided by the observer, are selected from the MIR spectro-photometric standard star catalog of the VLT (<http://www.eso.org/instruments/visir>). This catalog is based on the radiometric all-sky network of absolutely calibrated stellar spectra by Cohen et al.<sup>1</sup>. This list is supplemented by MIR

---

<sup>1</sup>Cohen et al., 1999, AJ 117, 1864

standards used by TIMMI2<sup>2</sup>. At present the standard star catalog contains 425 sources. Zero point fluxes (Jy) have been calculated for the VISIR filter set using transmission curves (Fig. 18), detector efficiency (Fig. 8) and atmosphere (Fig. 1) as shown in the corresponding Figures.

A PSF can be derived from these photometric standard star observations. However, it is not guaranteed that the accuracy is sufficient for deconvolution purposes. If the observer requires a specific PSF measurement she has to provide the corresponding acquisition and science OB.

Observations of photometric standards will be taken using the `VISIR_img_cal_AutoChopNod` template (Sect. 6) with the following settings:

```
SEQ.TIME          180s for N and 360 s for Q band
TEL.CHOP.POSANG   0°
TEL.CHOP.THROW    10''
SEQ.CHOPNOD.DIR   PERPENDICULAR
```

Filter `INS.FILT1.NAME` and pixel scale `INS.PFOV` will be set according to the science observations.

In spectroscopy, the observatory will provide spectro-photometric observation of a telluric standard star. Such a calibration measurement will be performed once per night, per instrument configuration. More precisely the following settings of the `VISIR_spec_cal_LRAutoChopNod` template (Sect. 6) will be used:

```
SEQ.TIME          300 s
TEL.CHOP.POSANG   0°
TEL.CHOP.THROW    10''
SEQ.CHOPNOD.DIR   PARALLEL
```

The wavelength setting `INS.GRAT1.WLEN` will be adjusted to the science observation.

#### Important note:

1. The observatory does only provide standard calibrations for low resolution spectroscopy in the 1''slit.
2. The observatory does **not** provide standard calibrations for VISIR medium and high resolution spectroscopy. Thus for medium and high resolution mode the observer has to supply his own calibration by attaching a calibration template to the science OB. The observing time needed to execute this calibration is charged to the observer. Ideally, early type stars should be chosen.

## 5 VISIR data

### 5.1 Data format

One FITS file is saved for each telescope nodding position. This file is a data cube and contains for each chopping cycle:

1. half cycle frames of the on source position (A) of the chopper,
2. the average of the current and all previous(A-B) chopped frames,
3. the average of all chopped frames, which is stored in the last plane of the data cube.

In the fits file images are oriented North up and East left and spectroscopic data are aligned horizontally in the spatial and vertically in the dispersion direction (cf. Fig.15).

<sup>2</sup><http://www.ls.eso.org/lasilla/sciops/3p6/timmi/html/stand.html>

## 5.2 Pipeline

The VISIR pipeline has been developed by ESO/DMD and uses the ESO/CPL library. The main observation templates are supported by the pipeline reductions. Raw images of imaging and spectroscopic observations are recombined. Spectra are extracted and calibrated in wavelength (Sect. 5.3) for the long-slit modes in low-, medium-, and high-resolution. Sensitivity estimates based on standard star observations are provided both in imaging and spectroscopy (Sect. 4.7).

The pipeline currently supports the following templates :

- VISIR\_img\_obs\_AutoChopNod
- VISIR\_spec\_obs\_LRAutoChopNod
- VISIR\_spec\_obs\_MRAutoChopNod
- VISIR\_spec\_obs\_HRAutoChopNod

In raster mode (VISIR\_img\_obs\_GenericChopNod) only raw frames are delivered, e.g. mapping reconstruction algorithms are not supported.

## 5.3 VISIR spectrometer data

### Optical distortion correction

Spectra are deformed by optical distortion and slit curvatures. The VISIR spectrograph uses curved slits to cancel the distortion of the pre-slit optics. Thus the slit projected on the sky is straight. There is an additional linear distortion in both dispersion and cross-dispersion direction of the detector. The following algorithm is supported by the pipeline for low and medium resolution mode. Let us define the detector pixels in dispersion direction by  $x$  and in cross-dispersion direction by  $y$ , respectively :

a) The skew angle along  $x$  with  $\Phi$  and along  $y$  with  $\Psi$ .

b) The maximum curvature along  $x$  with  $\Delta$  and along  $y$  with  $\epsilon$ .

$\Phi$  is defined positive in clockwise-direction and  $\Psi$  counter-clockwise;  $\Delta$  is positive by increasing  $x$  and  $\epsilon$  by decreasing  $y$ , respectively. Measured values of the distortion parameters are in the low and medium resolution mode  $\Phi = 1.6^\circ$  and  $\Psi = 0.7^\circ$ . The curvatures in the low resolution mode are  $\epsilon = 1.04$  pixel,  $\Delta = 0.08$  pixel and for the medium resolution mode are  $\epsilon = 0.26$  pixel,  $\Delta = 0.08$  pixel. The center of the lower left of the detector is at (1,1). Therefore, the fix point, which is the detector center, is at (128.5, 128.5) for the  $n = 256$  pixel array of the DRS.

The fix point is moved to (1,1) by:

$$f_1(x, y) = \left(x - \frac{n+1}{2}, y - \frac{n+1}{2}\right) \quad (6)$$

and the skew is corrected along the cross-dispersion:

$$f_2(x, y) = (x + y \cdot \tan(\Psi), y) \quad (7)$$

and along the dispersion direction:

$$f_3(x, y) = (x, y + x \cdot \tan(\Phi)) \quad (8)$$

The curvature is a segment of a circle with radius,  $R$  in  $x$ -direction given by:  $n = 2\sqrt{\epsilon \cdot (2R_\epsilon - \epsilon)}$  and in  $y$ -direction by:  $n = 2\sqrt{\Delta \cdot (2R_\Delta - \Delta)}$ . It is corrected along the cross-dispersion:

$$f_4(x, y) = (x, y - \text{sign}(\epsilon) \cdot (R_\epsilon - \sqrt{R_\epsilon^2 - x^2})) \quad ; \quad (\epsilon \neq 0) \quad (9)$$

and along the dispersion:

$$f_5(x, y) = (x + \text{sign}(\Delta) \cdot (R_\Delta - \sqrt{R_\Delta^2 - y^2}), y) \quad ; \quad (\Delta \neq 0) \quad (10)$$

Finally, the origin of the coordinate system is moved back from the fix point to (1,1):

$$f_6(x, y) = \left(x + \frac{n+1}{2}, y + \frac{n+1}{2}\right) \quad (11)$$

Spectral extraction is similar to the TIMMI2 pipeline and described by Siebenmorgen et al. 2004, AA 414, 123.

### **Wavelength calibration**

A first order wavelength calibration is given by the optical model of the instrument. Its precision is about  $\pm 10$  pixels for the low and medium resolution mode and  $\pm 15$  pixels for the high resolution mode. The wavelength calibration can be refined by using Fabry-Perot Etalons plates or atmospheric lines. In the VISIR FITS file, chopper half-cycle frames, which are dominated by sky emission lines, are stored (Sect.5.1). They can be used to fine-tune the wavelength calibration to sub-pixel precision by comparison with atmospheric lines. Wavelength calibration based on the atmospheric model is supported by the pipeline. The chopped frames cannot be used for calibration with atmospheric lines because the chopping process results in a near perfect cancelation of sky lines.

### **Fringing**

The DRS detector shows fringes which are generated in the detector substrate. One example of such fringes is shown in Fig. 15 for the low resolution mode. The fringes are stable and are not apparent in chopped images, but the spectra are modulated. Division of the extracted spectra by standard star spectra simultaneously removes most of the fringes and corrects for telluric features.

### **Atmosphere absorption correction**

The atmosphere does not uniformly absorb the MIR radiation (Sect. 2.1). At some wavelengths it is completely transparent, at others partly or completely opaque. Differential absorption is often corrected by dividing the extracted spectrum by a reference spectrum. This procedure may cause numerical instabilities at wavelengths close to strong sky lines that might amplify the noise.

### **Photometry**

Spectro-photometric calibration of low and medium resolution spectra can be achieved with the MIR standard star list provided by the Observatory (see Sect. 4.7). For high-resolution spectroscopy only calibrators known with high precision, such as, A stars or asteroids, should be considered. However, even early A stars are known to have some hydrogen absorption lines in the N and Q band.

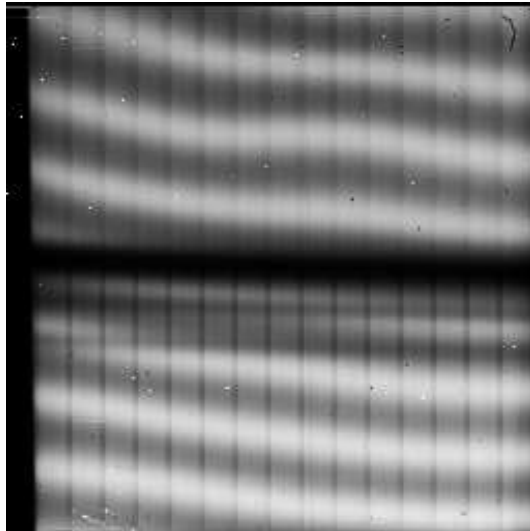


Figure 15: VISIR spectrum in staring, low-resolution mode showing the detector fringing (white). The detector absorption feature at  $8.8 \mu\text{m}$  is visible as black horizontal bar (cf. Fig. 8). Dark horizontal stripes are caused by the non-uniform gain of the different electronic amplifiers. These features are largely removed by chopping.

## 6 VISIR templates description

### 6.1 Acquisition

Each OB needs to start with an acquisition template, they are described in Sect. 4.3.

### 6.2 Observing with the imager

#### `VISIR_img_obs_AutoChopNod`

This template permits observing a source in imaging configuration with various sub-settings. The observer must specify filter, pixel scale, chopper throw, which is in the range of  $8''$  to  $30''$ . The keyword `SEQ.CHOPNOD.DIR` is set to `PARALLEL` or `PERPENDICULAR`, which results in images as shown in Fig. 16. `PARALLEL` considers an equal nodding and chopping amplitude which are both in parallel direction. It is recommended for faint, extended sources, for which the spatial resolution is not so crucial. `PERPENDICULAR` considers an equal nodding and chopping amplitude; however in perpendicular direction. Note that while the telescope offset is in positive (East) direction, the resulting image on the detector will move to the West. This technique is recommended for point or relatively small extended ( $< 5''$ ) sources (Fig. 3).

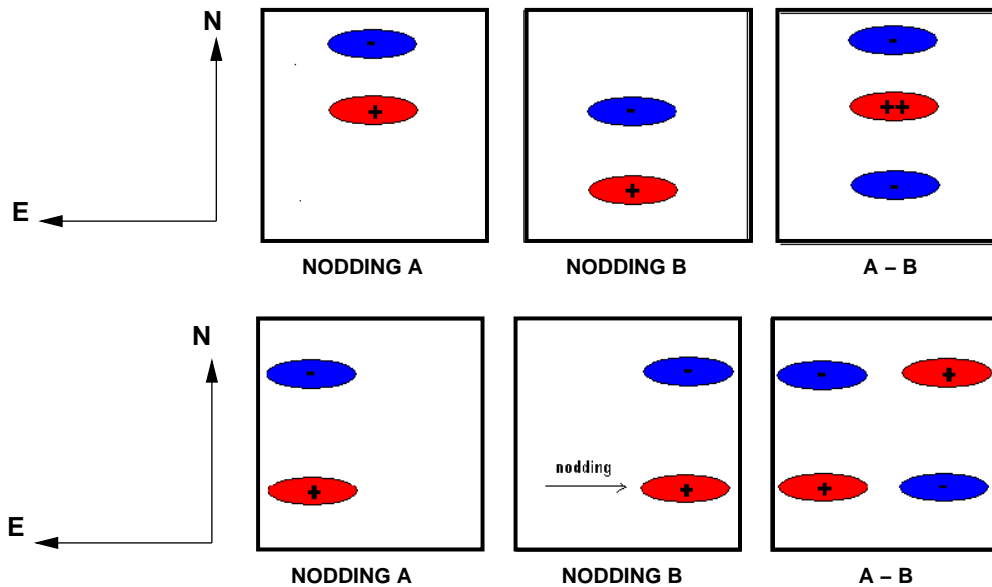


Figure 16: Schematic drawing of observation with `TEL.CHOP.POSANG = 0` and `SEQ.CHOPNOD.DIR = PARALLEL` (top) and `SEQ.CHOPNOD.DIR=PERPENDICULAR` (bottom).

The keywords `SEQ.JITTER.WIDTH` allows chopping and nodding with random offsets so that a jitter pattern is performed. This technique allows to reconstruct bad pixels. For `SEQ.JITTER.WIDTH= 0` no jitter is performed and the resulting image depends on the setting of `SEQ.CHOPNOD.DIR`. The chopping period is set by the system and the nodding period is fixed to 90s. The number of nodding cycles  $N_{cycl\_nod}$  is computed according to the total observation time (Sect. 3.5).

#### `VISIR_img_obs_GenericChopNod`

This imaging template enhances the flexibility of nodding offsets, and allows the user to specify them in a list of relative offset positions. In the most simple application, only one offset position is specified. This allows to record nodding pairs, i.e. cycle of on-off observations, using a flexible offset position. Additional jitter offsets can be specified. More than one entry in the offset list results in a freely programmable pattern of nodding pairs. Note that the integration time, `SEQ.TIME`, specified refers to only one nodding pair. The total observing time is given by the number of `SEQ.NOFF · SEQ.TIME`. The offset positions are calculated as the cumulative sum of offsets, i.e. are defined relative to the previous offset positions. Note that the telescope always returns to the first (reference) position, when specifying a list of offsets. This mode can be exploited to perform raster or map imaging. The first reference position can then be considered as a sky observation while the offsets refer to object positions. It is recommended to offset to positions that result in observations of overlapping fields, which enhances the redundancy after image reconstruction.



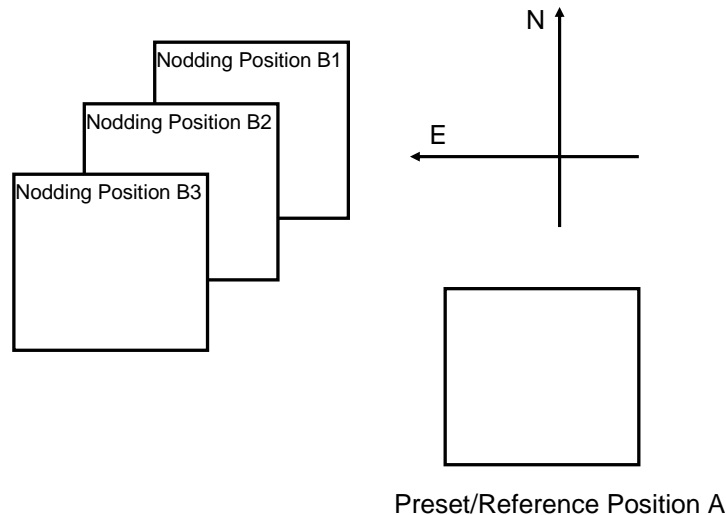


Figure 17: Illustration of generating raster maps with `VISIR_img_obs_GenericChopNod`.

An illustration of generating a raster map can be found in Fig. 17. The following parameters correspond to this setting:

```
SEQ.NOFF          3
SEQ.OFFSET1.LIST 30, 10, 10
SEQ.OFFSET2.LIST 30, -10, -10
SEQ.OFFSET.COORDS SKY
```

Note that depending on choice of the integration time `SEQ.TIME`, several nodding cycles might result, e.g. pattern like `AB1B1AAB1B1A..AB2B2AAB2B2A..AB3B3AAB3B3A`.

### 6.3 Observing with the spectrometer

Conceptually the same observing techniques applies for spectroscopy as well as for imaging. The default slit orientation is in North-South direction.

A preferred observing strategy is called "nodding on the slit", where the chopping and nodding amplitudes are small (`SEQ.CHOPNOD.DIR = PARALLEL`). Note that "nodding on the slit" requires to set the telescope rotator offset angle *and* the M2 chopping position angle to the same value (which is, in general, different from 0). This is useful to acquire two targets simultaneously in the slit.

More complex source geometries might require larger amplitudes, and/or `SEQ.CHOPNOD.DIR = PERPENDICULAR` in order to avoid self-cancellation.

#### Low and medium resolution

Templates for low and medium resolution spectroscopy are:

`VISIR_spec_obs_LRAutoChopNod` and `VISIR_spec_obs_MRAutoChopNod`, respectively. Observing parameters are: total integration time (`SEQ.TIME`), central wavelength (`INS.GRAT1.WLEN`) and `SEQ.CHOPNOD.DIR` (Sect.6.2).

#### High resolution

Template for high resolution spectroscopy is `VISIR_spc_obs_hrline`. In P75, the order sorting filter at  $12.8\mu\text{m}$ , `INS.FILT2.NAME = [Ne II]` is offered. Other observing parameters are: total integration time (`SEQ.TIME`), central wavelength (`INS.GRAT1.WLEN`) and `SEQ.CHOPNOD.DIR` (Sect.6.2).

## 6.4 Calibration

Specific templates exist for the observations of photometric and spectro-photometric standard stars. They offer the same functionality as the corresponding science templates, but allow to monitor the sensitivity and image quality by observing calibration standard stars.

## 7 Appendix: VISIR template parameters

### 7.1 Acquisition

VISIR-120.30/VISIR_img_acq_Preset.tsf		
<i>To be specified:</i>		
Parameter	Range (Default)	Label
<b>TEL.TARG.ALPHA</b>	ra ()	
<b>TEL.TARG.DELTA</b>	dec ()	
<b>TEL.TARG.EQUINOX</b>	(2000.0)	
<b>TEL.ROT.OFFANGLE</b>	0..359 (0.0)	Rotator on Sky (=PA on Sky)
<b>TEL.TARG.ADDVELALPHA</b>	(0.0)	RA additional tracking velocity
<b>TEL.TARG.ADDVELDELTA</b>	(0.0)	DEC additional tracking velocity
<b>TEL.AG.GUIDESTAR</b>	CATALOGUE SETUPFILE NONE (CATALOGUE)	Get Guide Star from
<b>TEL.GS1.ALPHA</b>	ra ()	Guide star RA
<b>TEL.GS1.DELTA</b>	dec ()	Guide star DEC

VISIR-120.30/VISIR_img_acq_MoveToPixel.tsf		
<i>To be specified:</i>		
Parameter	Range (Default)	Label
<b>SEQ.CHOPNOD.DIR</b>	PARALLEL PERPENDICU- LAR (PARALLEL)	Relative Chop/Nod Direction
<b>SEQ.TIME</b>	30..3600 (NODEFAULT)	Total integration time (sec)
<b>TEL.TARG.ALPHA</b>	ra ()	
<b>TEL.TARG.DELTA</b>	dec ()	
<b>TEL.TARG.EQUINOX</b>	(2000.0)	
<b>TEL.TARG.OFFSETALPHA</b>	(0.0)	RA blind offset
<b>TEL.TARG.OFFSETDELTA</b>	(0.0)	DEC blind offset
<b>TEL.ROT.OFFANGLE</b>	0..359 (0.0)	Rotator on Sky (=PA on Sky)
<b>TEL.TARG.ADDVELALPHA</b>	(0.0)	RA additional tracking velocity
<b>TEL.TARG.ADDVELDELTA</b>	(0.0)	DEC additional tracking velocity
<b>TEL.AG.GUIDESTAR</b>	CATALOGUE SETUPFILE NONE (CATALOGUE)	Get Guide Star from
<b>TEL.GS1.ALPHA</b>	ra ()	Guide star RA
<b>TEL.GS1.DELTA</b>	dec ()	Guide star DEC
<b>TEL.CHOP.POSANG</b>	0..359 (0)	Chopping Position Angle (deg)
<b>TEL.CHOP.THROW</b>	8..30 (10)	Chopping Amplitude (arcsec)
<b>INS.FILT1.NAME</b>	SIC PAH1 ARIII SIV_1 SIV SIV_2 PAH2 PAH2.2 NEII.1 NEII NEII.2 Q1 Q2 Q3 (NODE- FAULT)	Imager Filter
<b>INS.PFOV</b>	0.075 0.127 (0.127)	Imager pixel scale

VISIR-120.30/VISIR_spec_acq_MoveToSlit.tsf		
<i>To be specified:</i>		
Parameter	Range ( <i>Default</i> )	Label
<b>SEQ.CHOPNOD.DIR</b>	PARALLEL PERPENDICULAR ( <i>PARALLEL</i> )	Relative Chop/Nod Direction
<b>SEQ.TIME</b>	30..3600 ( <i>NODEFAULT</i> )	Total integration time (sec)
<b>TEL.TARG.ALPHA</b>	ra ()	
<b>TEL.TARG.DELTA</b>	dec ()	
<b>TEL.TARG.EQUINOX</b>	(2000.0)	
<b>TEL.TARG.OFFSETALPHA</b>	(0.0)	RA blind offset
<b>TEL.TARG.OFFSETDELTA</b>	(0.0)	DEC blind offset
<b>TEL.ROT.OFFANGLE</b>	0..359 (0.0)	Rotator on Sky (=PA on Sky)
<b>TEL.TARG.ADDVELALPHA</b>	(0.0)	RA additional tracking velocity
<b>TEL.TARG.ADDVELDELTA</b>	(0.0)	DEC additional tracking velocity
<b>TEL.AG.GUIDESTAR</b>	CATALOGUE SETUPFILE NONE ( <i>CATALOGUE</i> )	Get Guide Star from
<b>TEL.GS1.ALPHA</b>	ra ()	Guide star RA
<b>TEL.GS1.DELTA</b>	dec ()	Guide star DEC
<b>TEL.CHOP.POSANG</b>	0..359 (0)	Chopping Position Angle (deg)
<b>TEL.CHOP.THROW</b>	8..30 (10)	Chopping Amplitude (arcsec)
<b>INS.FILT2.NAME</b>	N_SW N_LW ARIII NEII.1 NEII.2 ( <i>NODEFAULT</i> )	Acquisition Filter
<b>INS.SLIT1.WIDTH</b>	0.40 0.75 1.00 ( <i>NODEFAULT</i> )	Spectrometer Slit Width (arcsec)

## 7.2 Observation

VISIR-120.30/VISIR_img_obs_AutoChopNod.tsf		
<i>To be specified:</i>		
Parameter	Range ( <i>Default</i> )	Label
<b>SEQ.CHOPNOD.DIR</b>	PARALLEL PERPENDICULAR ( <i>PARALLEL</i> )	Relative Chop/Nod Direction
<b>SEQ.JITTER.WIDTH</b>	0..10 (0)	Random Jitter Box Width (arcsec)
<b>SEQ.TIME</b>	180..3600 ( <i>NODEFAULT</i> )	Total integration time (sec)
<b>TEL.CHOP.POSANG</b>	0..359 (0)	Chopping Position Angle (deg)
<b>TEL.CHOP.THROW</b>	8..30 (10)	Chopping Amplitude (arcsec)
<b>INS.FILT1.NAME</b>	SIC PAH1 ARIII SIV_1 SIV SIV_2 PAH2 PAH2.2 NEII.1 NEII NEII.2 Q1 Q2 Q3 ( <i>NODEFAULT</i> )	Imager Filter
<b>INS.PFOV</b>	0.075 0.127 (0.127)	Imager pixel scale

VISIR-120.30/VISIR_img_obs_GenericChopNod.tsf		
<i>To be specified:</i>		
Parameter	Range (Default)	Label
<b>SEQ.JITTER.WIDTH</b>	0..10 (0)	Random Jitter Box Width (arcsec)
<b>SEQ.NOFF</b>	1..100 (NODEFAULT)	Number of offset positions
<b>SEQ.OFFSET.COORDS</b>	SKY DETECTOR (NODEFAULT)	Offset coordinates
<b>SEQ.OFFSET1.LIST</b>	(NODEFAULT)	List of offsets in RA or X
<b>SEQ.OFFSET2.LIST</b>	(NODEFAULT)	List of offsets in DEC or Y
<b>SEQ.TIME</b>	180..3600 (NODEFAULT)	Total integration time (sec)
<b>TEL.CHOP.POSANG</b>	0..359 (0)	Chopping Position Angle (deg)
<b>TEL.CHOP.THROW</b>	8..30 (10)	Chopping Amplitude (arcsec)
<b>INS.FILT1.NAME</b>	SIC PAH1 ARIII SIV_1 SIV SIV_2 PAH2 PAH2.2 NEII_1 NEII NEII.2 Q1 Q2 Q3 (NODEFAULT)	Imager Filter
<b>INS.PFOV</b>	0.075 0.127 (0.127)	Imager pixel scale

VISIR-120.30/VISIR_spec_obs_LRAutoChopNod.tsf		
<i>To be specified:</i>		
Parameter	Range (Default)	Label
<b>SEQ.CHOPNOD.DIR</b>	PARALLEL PERPENDICULAR (PARALLEL)	Relative Chop/Nod Direction
<b>SEQ.TIME</b>	180..3600 (NODEFAULT)	Total integration time (sec)
<b>TEL.CHOP.POSANG</b>	0..359 (0)	Chopping Position Angle (deg)
<b>TEL.CHOP.THROW</b>	8..30 (10)	Chopping Amplitude (arcsec)
<b>INS.GRAT1.WLEN</b>	8.8 9.8 11.4 12.4 (NODEFAULT)	Spectrometer Wavelength (microns)

VISIR-120.30/VISIR_spec_obs_MRAutoChopNod.tsf		
<i>To be specified:</i>		
Parameter	Range (Default)	Label
<b>SEQ.CHOPNOD.DIR</b>	PARALLEL PERPENDICULAR (PARALLEL)	Relative Chop/Nod Direction
<b>SEQ.TIME</b>	180..3600 (NODEFAULT)	Total integration time (sec)
<b>TEL.CHOP.POSANG</b>	0..359 (0)	Chopping Position Angle (deg)
<b>TEL.CHOP.THROW</b>	8..30 (10)	Chopping Amplitude (arcsec)
<b>INS.GRAT1.WLEN</b>	8.8 11.4 (NODEFAULT)	Spectrometer Wavelength (microns)

VISIR-120.30/VISIR_spec_obs_HRAutoChopNod.tsf		
<i>To be specified:</i>		
Parameter	Range (Default)	Label
<b>SEQ.CHOPNOD.DIR</b>	PARALLEL PERPENDICULAR ( <i>PARALLEL</i> )	Relative Chop/Nod Direction
<b>SEQ.TIME</b>	180..3600 ( <i>NODEFAULT</i> )	Total integration time (sec)
<b>TEL.CHOP.POSANG</b>	0..359 ( <i>0</i> )	Chopping Position Angle (deg)
<b>TEL.CHOP.THROW</b>	8..30 ( <i>10</i> )	Chopping Amplitude (arcsec)
<b>INS.FILT2.NAME</b>	NEII.2 ( <i>NEII_2</i> )	Spectrometer Filter
<b>INS.GRAT1.WLEN</b>	12.738..12.882 ( <i>12.810</i> )	Spectrometer Wavelength (microns)

### 7.3 Calibration

VISIR-120.30/VISIR_img_cal_AutoChopNod.tsf		
<i>To be specified:</i>		
Parameter	Range (Default)	Label
<b>SEQ.CHOPNOD.DIR</b>	PARALLEL PERPENDICULAR ( <i>PERPENDICULAR</i> )	Relative Chop/Nod Direction
<b>SEQ.JITTER.WIDTH</b>	0..10 ( <i>0</i> )	Random Jitter Box Width (arcsec)
<b>SEQ.TIME</b>	30..3600 ( <i>NODEFAULT</i> )	Total integration time (sec)
<b>TEL.CHOP.POSANG</b>	0..359 ( <i>0</i> )	Chopping Position Angle (deg)
<b>TEL.CHOP.THROW</b>	8..30 ( <i>10</i> )	Chopping Amplitude (arcsec)
<b>INS.FILT1.NAME</b>	SIC PAH1 ARIII SIV_1 SIV SIV_2 PAH2 PAH2.2 NEII.1 NEII NEII.2 Q1 Q2 Q3 ( <i>NODEFAULT</i> )	Imager Filter
<b>INS.PFOV</b>	0.075 0.127 ( <i>0.127</i> )	Imager pixel scale

VISIR-120.30/VISIR_spec_cal_LRAutoChopNod.tsf		
<i>To be specified:</i>		
Parameter	Range (Default)	Label
<b>SEQ.CHOPNOD.DIR</b>	PARALLEL PERPENDICULAR ( <i>PARALLEL</i> )	Relative Chop/Nod Direction
<b>SEQ.TIME</b>	30..3600 ( <i>NODEFAULT</i> )	Total integration time (sec)
<b>TEL.CHOP.POSANG</b>	0..359 ( <i>0</i> )	Chopping Position Angle (deg)
<b>TEL.CHOP.THROW</b>	8..30 ( <i>10</i> )	Chopping Amplitude (arcsec)
<b>INS.GRAT1.WLEN</b>	8.8 9.8 11.4 12.4 ( <i>NODEFAULT</i> )	Spectrometer Wavelength (microns)

VISIR-120.30/VISIR_spec_cal_MRAutoChopNod.tsf		
<i>To be specified:</i>		
Parameter	Range (Default)	Label
<b>SEQ.CHOPNOD.DIR</b>	PARALLEL PERPENDICULAR ( <i>PARALLEL</i> )	Relative Chop/Nod Direction
<b>SEQ.TIME</b>	30..3600 ( <i>NODEFAULT</i> )	Total integration time (sec)
<b>TEL.CHOP.POSANG</b>	0..359 ( <i>0</i> )	Chopping Position Angle (deg)
<b>TEL.CHOP.THROW</b>	8..30 ( <i>10</i> )	Chopping Amplitude (arcsec)
<b>INS.GRAT1.WLEN</b>	8.8 11.4 ( <i>NODEFAULT</i> )	Spectrometer Wavelength (microns)

VISIR-120.30/VISIR_spec_cal_HRAutoChopNod.tsf		
<i>To be specified:</i>		
Parameter	Range (Default)	Label
<b>SEQ.CHOPNOD.DIR</b>	PARALLEL PERPENDICULAR ( <i>PARALLEL</i> )	Relative Chop/Nod Direction
<b>SEQ.TIME</b>	30..3600 ( <i>NODEFAULT</i> )	Total integration time (sec)
<b>TEL.CHOP.POSANG</b>	0..359 ( <i>0</i> )	Chopping Position Angle (deg)
<b>TEL.CHOP.THROW</b>	8..30 ( <i>10</i> )	Chopping Amplitude (arcsec)
<b>INS.FILT2.NAME</b>	NEII.2 ( <i>NEII_2</i> )	Spectrometer Filter
<b>INS.GRAT1.WLEN</b>	12.738..12.882 ( <i>12.810</i> )	Spectrometer Wavelength (microns)

## 8 Appendix: Filter transmission curves

The filter transmission has been measured using a Fourier Transform Spectrometer, at a temperature of 35 K for filters manufactured by the company READING. Their absolute transmission curves are displayed in Fig. 18. The other filters, manufactured by OCLI, have also been measured using the WCU and wavelength scans with the monochromator. Note that for these filters, the presented transmissions are only relative, but normalized to 1, see Fig. 19.

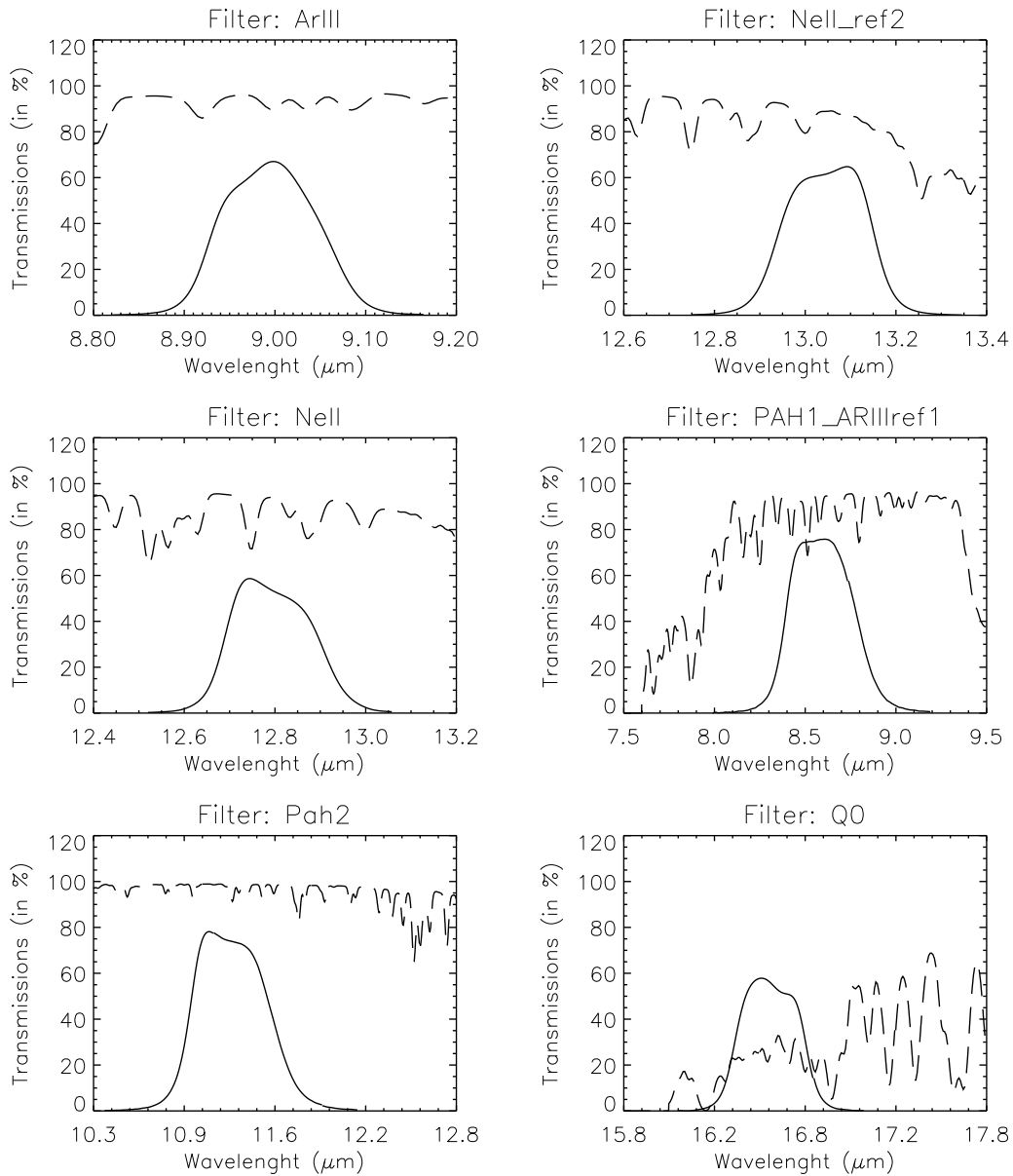


Figure 18: Transmission curves of VISIR imager filters, manufactured by READING. Overplotted (dashed) is the atmospheric transmission at low resolution. Note that the absolute transmission values are given, expressed in percent.



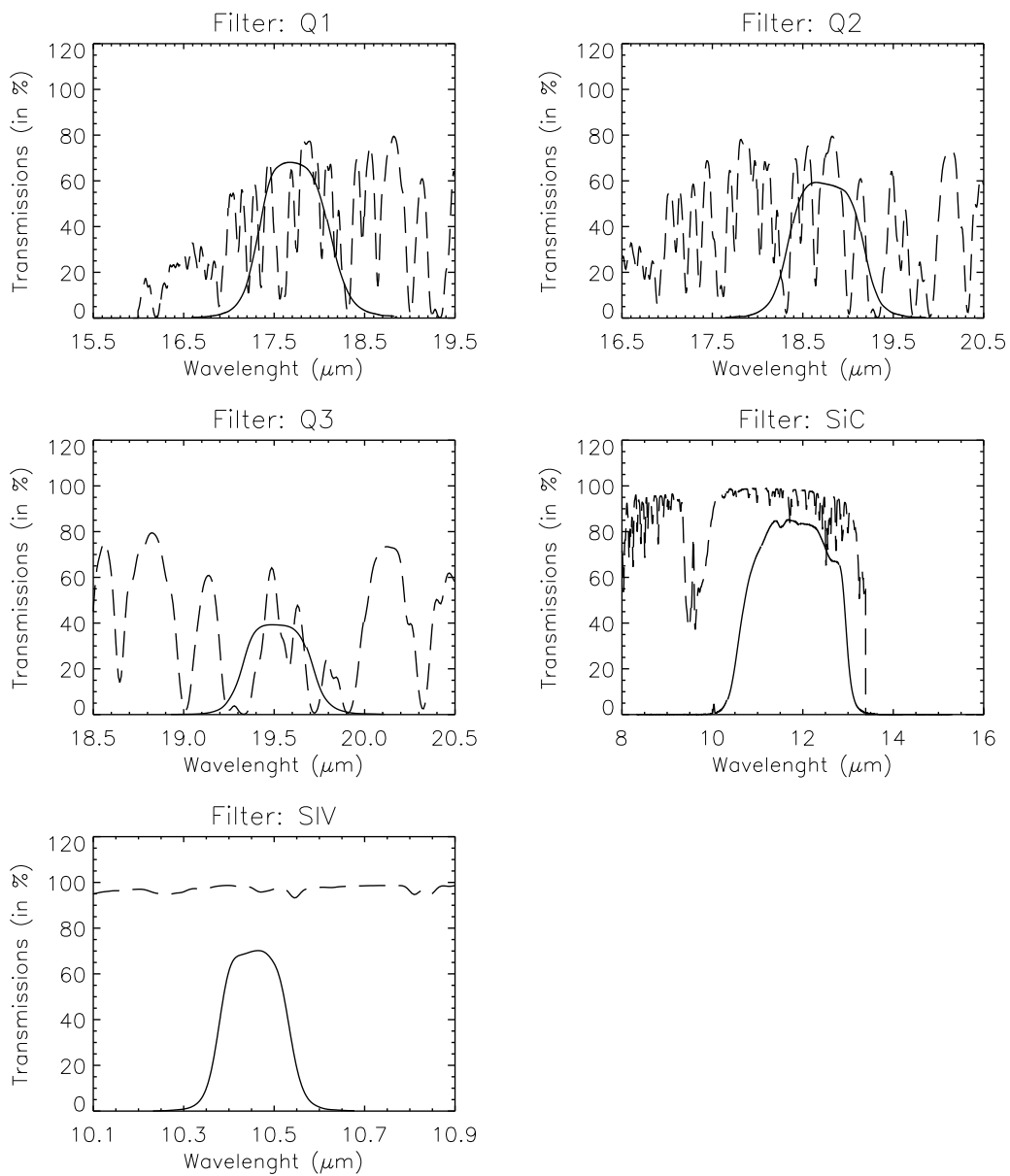


Figure 18: – continued.

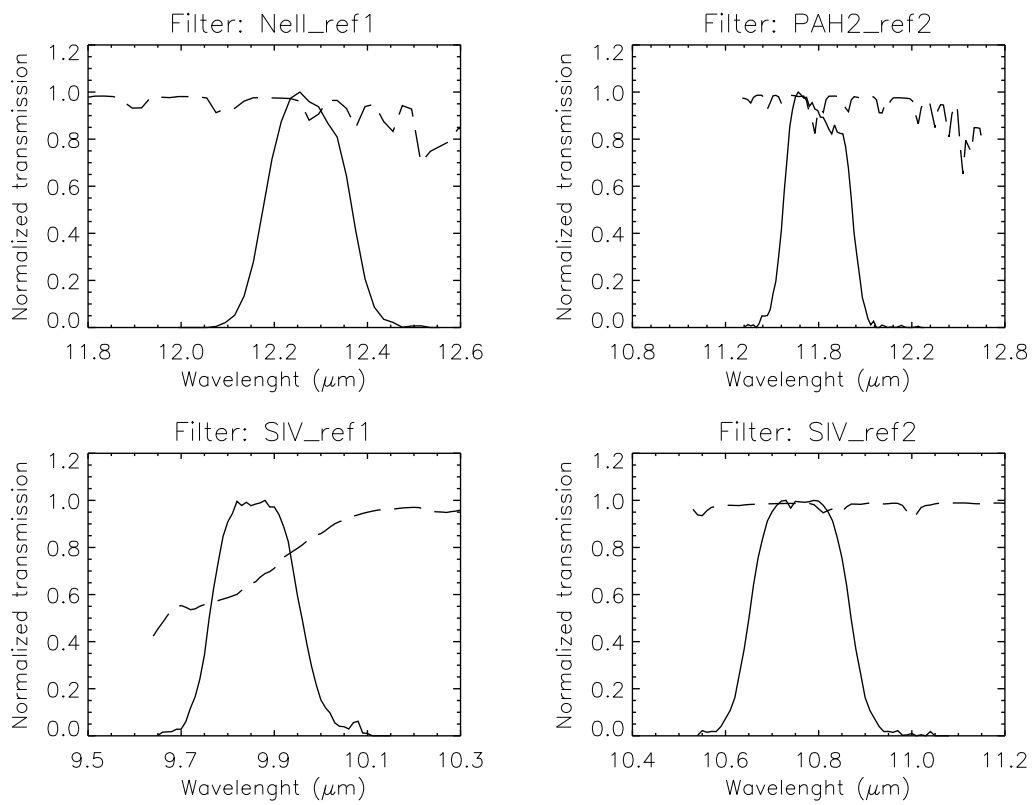


Figure 19: Transmission curves of VISIR imager filters, manufactured by OCLI. Overplotted (dashed) is the atmospheric transmission at low resolution. Note that only relative transmissions were determined; their values are displayed normalized to 1.